Chemical adsorption of NiO nanostructures on nickel foam-graphene for supercapacitor applications

A. Bello[1], K Makgopa[2], M. Fabiane[1], D. Dodoo-Ahrin[1], K.I. Ozoemena[2,3] and N. Manyala[1*]

[1]Department of Physics, Institute of Applied Materials, SARChI Chair in Carbon Technology and Materials, University of Pretoria, Pretoria 0028, South Africa

[2]Department of Chemistry, University of Pretoria, Pretoria 0002, South Africa

[3]Council for Scientific and Industrial Research, Pretoria South Africa, Meiring Naude Road, Brummeria, 395 Pretoria, 0001, South Africa

Corresponding author. N Manyala.

E-mail address: ncholu.manyala@up.ac.za

Tel: +27 (0)12 420 3549, Fax: +27 (0)12 420 2516

Abstract

Few-layer graphene was synthesized on a nickel foam template by chemical vapour deposition (CVD). The resulting three-dimensional (3D) graphene was loaded with nickel oxide nanostructures using the successive ionic layer adsorption and reaction (SILAR) technique. The composites were characterized and investigated as electrode material for supercapacitors. Raman spectroscopy measurements on the sample revealed that the 3D graphene consisted of mostly few layers, while X-ray diffractometry (XRD) and scanning electron microscopy (SEM) revealed the presence of nickel oxide. The electrochemical properties were investigated using cyclic voltammetry, electrochemical impedance spectroscopy and potentiostatic charge-discharge in aqueous KOH electrolyte. The novelty of this work is the use of the 3D porous cell structure of the nickel foam which allows for the growth of highly conductive graphene and subsequently provides support for uniform adsorption of the NiO onto the graphene. The NF-G/NiO electrode material showed excellent properties as a pseudocapacitive device with a high specific capacitance value of 783 Fg^{-1} at a scan rate of 2 mVs^{-1}. The device also exhibited excellent cycle stability, with 84% retention of the initial capacitance after 1,000 cycles. The results demonstrate that composites made using 3D graphene are versatile and show considerable promise as electrode materials for supercapacitor applications.

Keywords: Nickel foam-graphene; CVD; NiO; SILAR; Supercapacitor.

Introduction

Supercapacitors are electrochemical capacitors (ECs) that have received considerable attention because of their excellent properties which include high power density, long cycle life, low temperature sensitivity, low maintenance cost and their environmentally friendly nature [1-3]. Depending on the charge storage mechanism of the material, supercapacitors are classified as either electrochemical double layer capacitors (EDLCs) using ion adsorption, or pseudocapacitors using a fast and reversible Faradic reaction. They fill the gap between batteries (which have high energy density) and electrolytic capacitors (which have high power density) [4]. However, the energy stored in supercapacitor devices (<10 $Whkg^{-1}$) is low compared with that of batteries (>100 $Whkg^{-1}$). This has posed significant and difficult challenges in employing supercapacitors as primary power sources for battery replacement [5, 6]. It has also restricted the use of supercapacitors for possible applications such as in memory back-up equipment, hybrid vehicles, cordless electric tools, cellular phones and entertainment instruments [7]. Carbon-based materials such as activated carbon have been used as electrode material for EDLCs because of their high surface area and conductivity, while conducting polymers or transition metal oxides, as active electrode materials, have been used as pseudocapacitors [8, 9].

Graphene, a two-dimensional honeycomb lattice of sp^2-bonded carbon atoms, has emerged as an exciting material with numerous applications and has thus attracted intense research activity [10-12]. More recently, it has been explored for electrochemical storage applications due to its high surface area (2,630 m^2g^{-1}), high electrical conductivity, chemical stability and excellent mechanical properties [13-17]. However, graphene sheet has a tendency to restack due to the strong π-π bonds between the layers forming the graphite during the preparation of electrodes, thereby leading to inferior electronic properties for graphene-based supercapacitors. This drastically affects the performance of the supercapacitors [15]. To overcome this problem, fillers or pseudocapacitive materials can be introduced into the graphene layers which ultimately prevent restacking of the graphene and ensure maximum utilization of the graphene surface area, as well as contributing to the total specific capacitance of the system [18].

Nickel oxide (NiO) is one of the transition metal oxides that have attracted much attention as an electrode material for electrochemical capacitors because of its high theoretical capacitance (pseudocapacitance), multiple reversible electrochemical reactions, high surface-to-volume ratio, and because it is inexpensive and easy to synthesize [19-22]. Recently, several techniques for the preparation, characterization and application of various shapes and dimensions of NiO nanostructure for electrochemical applications have

been reported. Techniques such as self-assembly [19], electrochemical preparation [23], hydrothermal preparation [24, 25], chemical bath deposition [26] and chemical solution processes [27, 28] have all been investigated.

Chen et al. [29] recently reported growing 3D flexible and conductive interconnected graphene networks by chemical vapour deposition (CVD) using a nickel foam template. Such a graphene provides a highly conductive network due to the high intrinsic conductivity of defect-free graphene. The porous nature of the 3D network makes it an excellent platform for the incorporation of various nanoparticles or fillers to occupy the pore spaces for composite applications. Hence 3D graphene has been considered an important component of various composite materials, especially of graphene/metal oxide composites. Dong et al. [30] also reported the preparation of a novel 3D graphene network with NiO using the potentiostatic electrodeposition method. A specific capacitance of 816 Fg^{-1} was recorded at a scan rate of 5 mVs^{-1} for the graphene/NiO composite. Since then, several composites of 3D graphene foam have been investigated. For example, hybrid structures of zinc oxide nanorods on 3D graphene foam for supercapacitors and electrochemical sensor applications have also been reported [31], as well as electrodeposition of platinum particles on 3D interconnected graphene for fuel cell applications [32], and 3D graphene cobalt oxide electrodes for high-performance supercapacitors and enzymeless glucose detection [33]. Preparation of a nickel-foam-supported graphene sheet/porous NiO hybrid film by the combination of electrophoretic deposition and chemical-bath deposition was also investigated [34], and 3D flower-like NiO on graphene sheets was evaluated using a facile hydrothermal process and thermal treatment approach [35]. In addition, composite electrodes for supercapacitors were fabricated by impregnation of slurries of manganese dioxide nanofibres and multiwalled carbon nanotubes into porous nickel foam current collectors [36].

In this paper we have employed SILAR (successive ionic layer adsorption and reaction), a well-known, simple and reproducible chemical method, to synthesize novel nickel foam-graphene/nickel oxide (NF-G/NiO) in which the NiO nanostructures are anchored uniformly onto the surface of the graphene. The introduction of NiO into the graphene layers was expected to make maximum use of the surface area of the graphene and prevent agglomeration and restacking of the graphene sheet, thereby leading to improved conductivity of the composite and excellent electrochemical performance. The NF-G/NiO composite exhibited 3D porous interconnected network structure and was then tested as an electrode material for supercapacitors. The unique electrode structure not only enhanced easy access to ions from the electrolyte at the electrode/electrolyte interface, but also served as a platform for the combination and integration of NiO with and into the NF-G.

Experimental procedure

Graphene foam was synthesized by chemical vapour deposition onto a catalytic nickel foam (Alantum, Munich, Germany), 420 g/m^2 in areal density and 1.6 mm in thickness. The nickel foam was annealed at 800 ^{o}C in the presence of Ar and H_2 for 20 min to remove impurities, before the introduction of the CH_4 gas at 1000 ^{o}C. The flow rates of the gases (CH_4:H_2:Ar) were 10 sccm:200 sccm:300 sccm respectively. After 5 min of deposition, the sample was rapidly cooled by pushing the quartz tube to a lower temperature region. The deposition of NiO onto the substrate (nickel foam-graphene) was done using the SILAR method. This is a stepwise chemical deposition technique based on immersion of the substrate into separately placed cationic and anionic precursors and rinsing after every immersion cycle with deionized water to avoid homogeneous precipitation [37-39]. The cationic precursor for this work was a mixture of 0.01 M $Ni(NO_3)_2.6H_2O$ and aqueous ammonia. Initially, precipitate of $Ni(OH)_2$ was formed from 0.01 M $Ni(NO_3)_2.6H_2O$, which was dissolved upon addition of ammonia to adjust the pH to ~12, thereby forming hexa-amminonickel (II) complex. The anionic precursor source was a hot water bath. When the substrate was immersed in the precursor solution (0.01 M $Ni(NO_3)_2.6H_2O$) at room temperature for 30 s, nickel ions were adsorbed onto the substrate surface. The substrate was then transferred to the hot water bath at a temperature of 90 ºC for another 30 s to convert it into NiO, after which it was rinsed in distilled water for 30 s to remove the loosely bound or excess nickel hydroxyl ions. The SILAR steps were repeated for 60 cycles. After deposition, the samples were dried at 50 ºC in an oven for about 1 h. Typically, the NF-G/NiO composite contained 26 wt.% NF-G and 74 wt.% NiO. The important parameters in the SILAR technique are the concentration and pH of the precursor solution, the temperature and the time for adsorption and rinsing.

Raman spectroscopy data were collected using a Jobin Yvon Horiba TX 6400 micro-Raman spectrometer equipped with a triple monochromator system to eliminate contributions from Rayleigh scattering. The samples were analyzed with a 514 nm argon excitation laser (1.5 mW laser power on the sample to avoid thermal effects), using a × 50 objective with recording times ranging from 120 s. X-ray diffraction (XRD) patterns of the samples were collected using an XPERT-PRO diffractometer (PANalytical BV, Netherlands) with theta/theta geometry, operating a cobalt tube at 35 kV and 50 mA. The goniometer is equipped with an automatic divergence slit and a PW3064 spinner stage. The instrumental resolution function was characterized with the NIST SRM 660a (LaB6) standard. The XRD pattern of all the samples was recorded in the 20.0^o-80^o 2θ, range with a step size of 0.017^o and a counting time of 15.240 s per step. Qualitative phase analysis of the samples was conducted using X'pert Highscore search-match software. Surface morphology characterization of

the samples was obtained using a high-resolution Zeiss Ultra Plus 55 field emission scanning electron microscope (FE-SEM) operated at 2.0 kV. The capacitive properties were investigated by the cyclic voltammetry (CV) method using an Autolab PGSTAT Workstation 302 (ECO-CHEMIE, Metrohm Autolab BV) driven by the GPES software. The as-prepared NF-G/NiO served as the working electrode, glassy carbon plate as the counterelectrode and Ag/AgCl (3M KCl) as the reference electrode in 2 M KOH electrolyte. Electrochemical impedance spectroscopy (EIS) was performed in the frequency range of 100 kHz - 1 MHz.

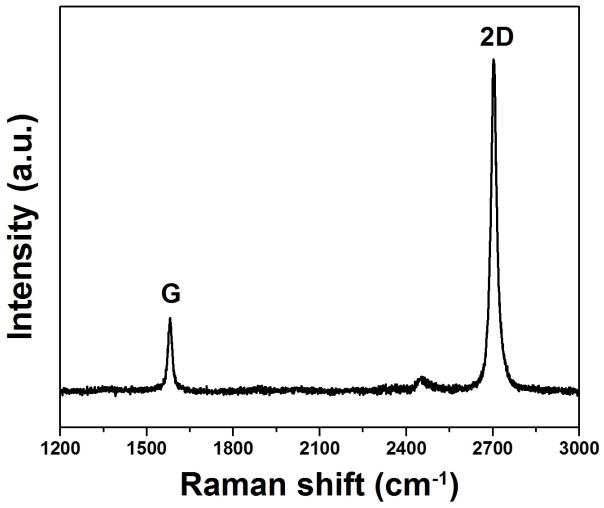

Fig. 1 Raman spectrum of graphene on nickel foam showing the G and the 2D bands, with the absence of the D band at 1350 cm^{-1}

Results and discussion

Fig. 1 shows the Raman spectrum of the graphene on the nickel foam. The spectrum has two major peaks corresponding to the first-order bond stretching G band at ~1581cm^{-1} and two phonon 2D bands at ~2702 cm^{-1}. The shape of the 2D bands, the I_{2D}/I_G ratio and the FWHM indicate that the graphene consists of mostly few layers. The absence from the spectrum of the D-peak (disorder) at 1350 cm^{-1} shows that the graphene is free from defects [40]. The XRD patterns of the nickel foam, nickel foam-graphene and nickel foam-graphene coated with NiO are shown in Fig. 2(a). All three strong peaks originated from the Ni foam, with the peaks belonging to graphene and NiO being invisible because they overlap with the Ni foam peaks. To confirm the presence of graphene and NiO in the sample, the same experiment was repeated for an etched sample where the nickel was removed and the graphene foam was coated with NiO. The two diffraction peaks at $2\theta = 31^o$ and 65^o shown in Fig. 2(b) correspond respectively to the (002) and (004) reflections of hexagonal

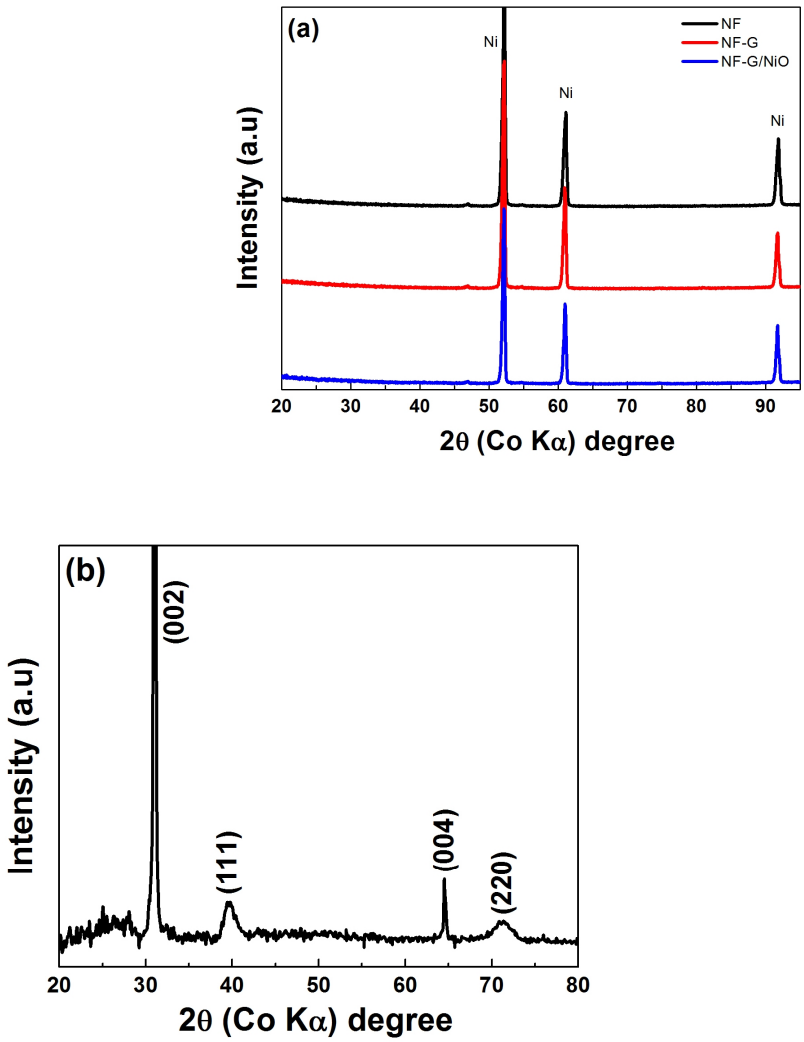

Fig. 2 XRD patterns of (a) nickel foam (NF), nickel foam-graphene (NF-G) and nickel foam-graphene/NiO (NF-G/NiO) and (b) graphene foam/NiO (GF/NiO) showing the presence of NiO in the sample

graphitic carbon, which is an indication of the presence of graphene, while the peaks labeled (111) and (220) in the same figure belong to NiO.

The SEM micrographs of the as-grown nickel foam-graphene are shown in Figs 3(a) and (b). Fig. 3(a) shows the porous structure of the nickel foam, while the micrograph in Fig. 3(b) of the same sample at higher magnification shows graphene wrapped around the Ni foam and reveals that the graphene consists of wrinkles and ripples which could be attributed to the different thermal expansion coefficients of Ni and graphene during the CVD synthesis [41, 42]. Fig. 3(c) shows a SEM image of the NF-G coated with NiO. It can be seen that the NiO nanostructures successfully coat the entire surface area of the NF-G, thus forming a porous and continuous

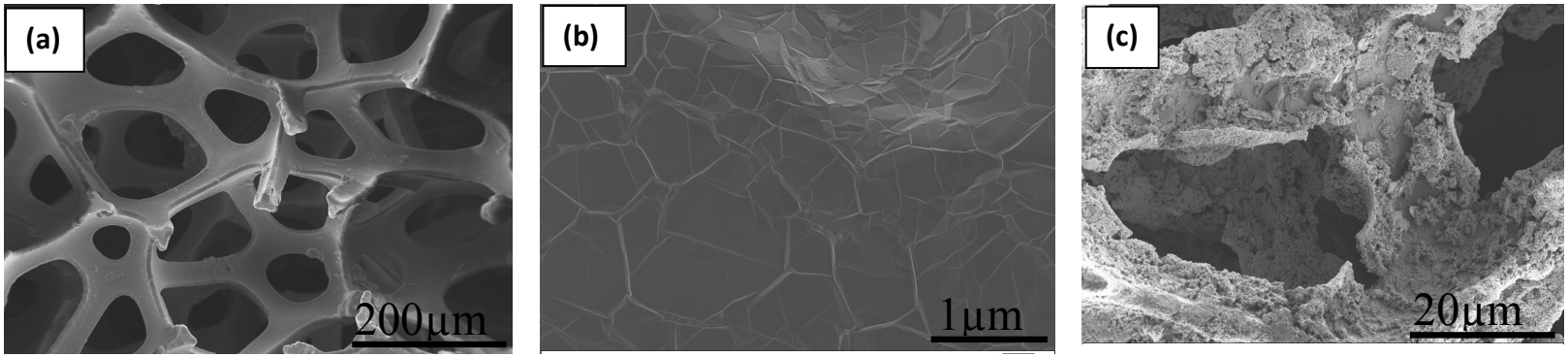

Fig. 3 SEM images of (a, b) NF-G at different magnifications revealing the 3D network and wrinkled structure of the graphene and (c) NF-G coated with NiO showing the NiO nanostructure uniformly anchored onto the surface of the graphene

electro-conductive network structure. This unique structure or morphology makes it useful in electrochemical capacitors, leading to pseudocapacitance when ions are adsorbed onto the surface of the samples and thereby improving capacitive behavior. It also provides an excellent electrode-electrolyte interface for the exchange of ions from the electrolyte.

Cyclic voltammetry studies were performed at various scan rates in a potential window of 0 V to 0.5 V to evaluate the capacitive behavior of the electrode materials. Fig. 4(a) compares the CV curves of samples at a scan rate of 10 mVs^{-1}. The shapes of the curves differed from those of ideal electrochemical double-layer capacitance, showing two redox peaks which are responsible for the pseudocapacitive behavior of the electrode materials. The oxidation peak observed at 0.419 V is due to the conversion of NiO to NiOOH, while the reduction peak at 0.192 V is due to the reverse reaction [39, 43] as represented by Equation (1) below:

$$NiO+OH^- \leftrightarrow NiOOH+e^- \quad (1)$$

The low-intensity current peaks observed in the NF-G sample are also due to the redox reaction of the nickel foam in the electrolyte [34]. However, the current response of NF-G/NiO is much higher than those of NF-G and NF-NiO, which is an indication that the NF-G/NiO electrode has a better capacitive performance than NF-G alone. This can be attributed to the fully utilized surface area of the graphene which provided support for uniform coating and loading of NiO in the samples.

The cyclic voltammetric curves of the NF-G/NiO electrode at different scan rates are shown in Fig. 4(b). It can be seen that the CV current response of the sample increases gradually with increasing scan rate; all CVs show a typical pseudocapacitive behavior. Fig. 4(c) compares the first discharge curves of the NF-G and NF-G/NiO at a current of 3 mA. They also show non-linear behavior, demonstrating the redox process of the NiO on the NF-G (i.e. pseudocapacitance). This is in agreement with the cyclic voltammogram in Fig. 4(a).

Fig. 4(d) shows a plot of the specific capacitance as a function of the scan rate, in which the specific capacitance decreases with increasing scan rate. This observation is an indication of a good current response of the NF-G/NiO and the pseudocapacitive nature of the electrode material, which is also consistent with the shapes of the CV curves. The specific capacitance (C_s) value can be calculated from either the CV measurement or the charge-discharge using either Equation 2 or Equation 3 below.

$$C_s = \frac{\bar{i}}{v \times m} \quad (2)$$

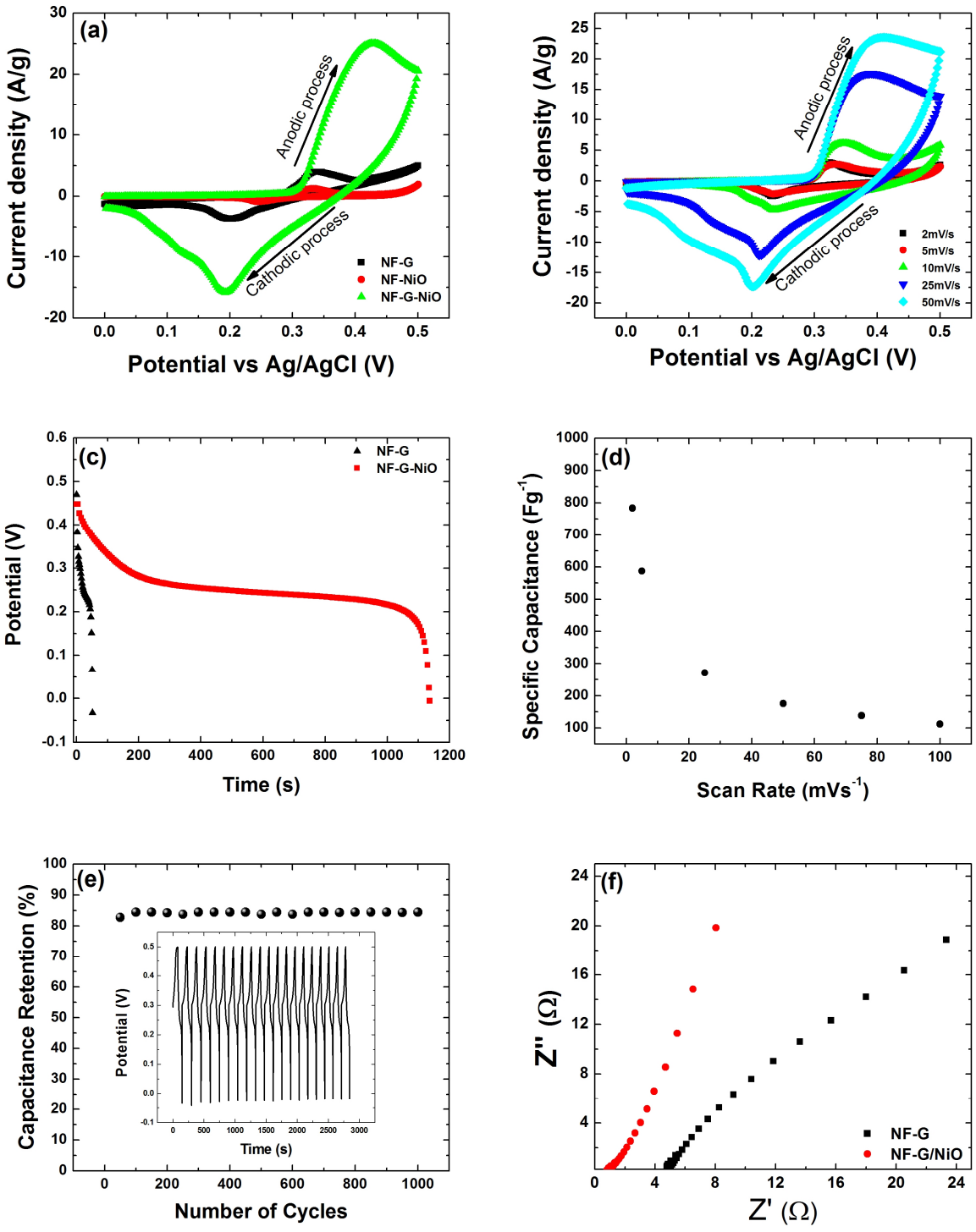

Fig. 4 Electrochemical measurements of the NF-G/NiO composites: (a) comparison of the CV curves of NF, NF-G and NF-G/NiO at a scan rate of 10 mVs^{-1}; (b) cyclic voltammetry curves of NF-G coated with NiO at scan rates of 2, 5, 10, 25 and 50 mVs^{-1}; (c) discharge curves for both samples at a current density of 3 mA; (d) specific capacitance as a function of scan rates for NF-G/NiO; (e) capacitance retention of the electrode material at a high current density of 10 mA; and (f) EIS (Nyquist) plots of both NF-G and NF-G/NiO

$$C_s = \frac{I \times \Delta T}{\Delta V} \quad (3)$$

where $\bar{i}$ is the average current (A), ν is the scan rate (mV/s), m is the mass of the electrode (g), I is the current, ΔT is the discharge time and ΔV is the discharge voltage.

Using Equation (2), a specific capacitance of 261 Fg^{-1} at 2 mVs^{-1} was obtained for the NF-G, while specific capacitances of 783 Fg^{-1} and 112 Fg^{-1} were obtained at 2 mVs^{-1} and 100 mVs^{-1} respectively for NF-G/NiO. Using Equation (3), a specific capacitance of 813 Fg^{-1} was obtained at a low current of 3 mA from the discharge curve for NF-G/NiO, which is closer to the specific capacitance that was obtained from the CV at a scan rate of 2 mVs^{-1}. These values are higher than those previously reported for G/NiO composites [34], but similar to those that Dong et al. [30] reported at a scan rate of 5 mVs^{-1} for graphene foam/NiO composite where the nickel template was etched away. This can be attributed to the high conductivity of 3D graphene sheets and the successful loading of NF-G/NiO by the SILAR method, resulting in improved electrochemical performance of the composite. Fig. 4(e) shows the continuous charge-discharge curve of the NF-G/NiO composite and the capacitance retention at a high current of 10 mA; the electrode is stable after 1,000 cycles and retains 84% of its initial capacitance.

EIS is a very powerful tool used to investigate the electrochemical characteristics of the electrode/electrolyte interface using a Nyquist plot, which is a representation of the real and imaginary parts of the impedance in a sample. The Nyquist plots of both NF-G and NF-G/NiO are shown in Fig. 4(f). The intercept in the high frequency region on the x-axis corresponds to the resistance of the electrolyte solution (R_s), and is also referred to as the equivalent series resistance (ESR), which consists of the resistance of the aqueous electrolyte, the intrinsic resistance of the composite material and the contact resistance at the electrode interface. The ESR values for the NF-G and NF-G/NiO electrodes were 4.8 Ω and 0.9 Ω respectively, as observed from Fig. 4(f). It is worth stating that for ideal supercapacitors, the EIS (Nyquist) plot should be a line perpendicular to the real axis at low frequency. However, comparing both samples, the Nyquist plot of NF-G/NiO is much closer to the ideal behavior due to the low charge transfer of graphene and NiO, thus indicating a better capacitive behavior. This improved electrochemical performance is due to the synergistic effect between graphene and NiO, leading to improved conductivity of the composite and a decrease in the internal resistance of the electrode. The 3D porous network structure of the nickel foam also helps to provide easy access to ions from the electrolyte at the electrode/electrolyte interface.

Conclusions

Graphene has been synthesized on nickel foam using CVD. The feasibility of using the successive ionic layer adsorption and reaction method (SILAR) to deposit nickel oxide onto the substrate (NF-G) has been tested. The results of the electrochemical experiments indicate that the as-grown NF-G when coated with NiO nanostructure exhibits good pseudocapacitive behavior. This is attributed mainly to the 3D nature of the NF which allows for 3D graphene growth, incorporation of NiO and combination with the conductivity of the graphene, leading to improved capacitance. The results show that nickel foam can be used directly for the growth of graphene and for electrochemical applications, rather than removing the nickel template which often introduces impurities into the sample from the etching agent. Furthermore, the open network structure of the composite makes it easily accessible for electrolyte movement and ion exchange during electrochemistry. The results obtained demonstrate that the nickel foam-graphene composite could be a promising material for accommodating metal oxide materials for electrochemical applications.

Acknowledgements

This work is based on research supported by the South African Research Chairs Initiative of the Department of Science and Technology (SARChI-DST) and the National Research Foundation (NRF). Any opinions, findings and conclusions or recommendations expressed in this work are those of authors and therefore the NRF and DST do not accept any liability with regard thereto. A.B thanks University of Pretoria and the NRF for

financial support for his study. K.M also thanks the NRF for a scarce-skills scholarship. We thank Dr Patricia Forbes for supplying the nickel foams.

References

[1] Conway BE (1999) Electrochemical supercapacitors: scientific fundamentals and technological applications, Kluwer Academia/Plenum Publishers, New York

[2] Kotz R, Carlen M (2000) Electrochim Acta 45:2483-2498

[3] Zaho X, Sánchez BM, Dobson PJ, Grant PS (2011) Nanoscale 3:839-855

[4] Hall PJ, Mirzaeian M, Fletcher SI, Sillars FB, Rennie AJR, Shitta-Bey GO, Wilson G, Cruden A, Carter R (2010) Energy Environ Sci 3:1238-1251

[5] Frackowiak E (2007) Phys Chem Chem Phys 9:1774-1785

[6] Burke A (2007) Electrochim Acta 53:1083-1091

[7] Frackowiak E, Benguin F (2001) Carbon 39:937-950

[8] Simon P, Gogotsi Y (2008) Nat Mater 7:845-854

[9] Zhang LL, Zhao XS (2009) Chem Soc Rev 38:2520-2531

[10] Geim AK, Novoselov KS (2007) Nat Mater 6:183-191

[11] Katsnelson MI (2007) Mater Today 10:20-27

[12] Novoselov KS, Geim AK, Morozov SV, Jiang D, Katsnelson MI, Grigorieva IV, Dubonos SV, Firsov AA (2004) Science 306:666-669

[13] Stoller MD, Park S, Zhu Y, An J, Ruoff RS (2008) Nano Lett 810:3498-3502

[14] Wang Y, Shi Z, Huang Y, Ma Y, Wang C, Chen M, Chen YS (2009) J Phys Chem C 113:13103-13107

[15] Liu C, Yu Z, Neff D, Zhamu A, Jang BZ (2010) Nano Lett 10:4863-4868

[16] Zhu Y, Murali S, Cai W, Li X, Suk JW, Potts JR, Ruoff RS (2010) Adv Mater 22:3906-3924

[17] Sun Y, Wu Q, Shi G (2011) Energy Environ Sci 4:1113-1132.

[18] Yu DS, Dai LM (2010) J Phys Chem Lett 1:467-470

[19] Yuan C, Zhang X, Su L, Gao B, Shen L (2009) J Mater Chem 19:5772-5777

[20] Xi YY, Li D, Djurisic AB, Xie MH, Man KYK, Chan WK (2008) Electrochem Solid-State Lett 11:D56-D59

[21] Konstantinov K, Wang G, Lao ZJ, Liu HK, Devers T (2009) J Nanosci Nanotech 9:1263-1267

[22] Bi RR, Wu XL, Cao FF, Jiang LY, Guo YG, Wan LJ (2010) J Phys Chem C:114 2448-2451

[23] Liang K, Tang X, Hu W (2012) J Mater Chem 22:11062-11067

[24] Li J, Zhao W, Huang F, Manivannanc A, Wu N (2011) Nanoscale 3:5103-5109

[25] Zhong W, Yun H, Xin-bo Z (2012) J Electrochem 18:151-156

[26] Xia XH, Tu JP, Wang XL, Gu CD, Zhao XB (2011) J Mater Chem 21:671-679

[27] Xia C, Yanjun X, Ning W (2011) Sens Actuators B 153:434-438

[28] Zhang X, Shi W, Zhu J, Zhao W, Ma J, Mhaisalkar S, Maria TL, Yang Y, Zhang H, Hang HH, Yan Q (2010) Nano Res 9:643-652

[29] Chen Z, Ren W, Gao L, Liu B, Pei S, Cheng H (2011) Nat Mater 10:424-428

[30] Dong X, Wang X, Wang L, Song H, Zhang H, Huang W, Chen (2012) Appl Mater Interfaces 4:3129-3133

[31] Cao X, Shi Y, Shi W, Lu G, Huang X, Yan Q, Zhang Q, Zhang H (2011) Small 7:3163-3168

[32] Xiaochen D, Yunfa C, Jing W, Mary BC, Lianhui W, Wei H, Chen P (2012) RSC Adv 2:4364-4369

[33] Thandavarayan M, Xiaochen D, Peng C, Xin W (2012) J Mater Chem 22:5286-5290

[34] Xia X, Tu J, Mai Y, Chen R, Wang X, Gu C, Zhao X (2011) J Chem Eur 17:10898-10905

[35] Ge C, Hou Z, Zeng BH, Cao J, Liu Y, Kuan Y (2012) J Sol-Gel Sci Technol 631:146-152

[36] Li J, Yang QM, Zhitomirsky I (2008) J Power Sources 185:1569-1574

[37] Lokhande CD Sankapala BR, Pathana HM, Mullerb M, Giersigb M, Tributsch H (2001) Appl Surf Sci 181:277-282

[38] Chung J, Myoung J, Oh J, Lim SJ (2012) Phys Chem Solids 73:535-539

[39] Wu M, Wang M, Jow J (2010) J Power Sources 195:3950-3955

[40] Ferrari AC (2007) Solid State Commun 143:47-57

[41] Wu M, Huang C, Lin K (2009) J Power Sources 186:557-564

[42] Chae SJ, Güneş F, Kim KK, Kim ES, Han GH, Kim SM, Shin H, Yoon S, Choi JY, Park MH, Yang CW, Pribat D, Lee YH (2009) Adv Mater 21:2328-2333

[43] Xing W, Li F, Yan Z, Lu G.Q (2004) J Power Sources 134:324-330